Influence of hydrogen in solution on the magnetism of monocrystalline thulium

1989 J. Phys.: Condens. Matter 1 4099

(http://iopscience.iop.org/0953-8984/1/26/006)

J. Phys.: Condens. Matter 1 (1989) 4099–4109. Printed in the UK

Influence of hydrogen in solution on the magnetism of monocrystalline thulium

P Vajda†, J N Daou†, J P Burger†, G Hilscher‡ and N Pillmayr‡

† Unitée associée au CNRS 803, 'Hydrogène dans les Métaux', Bâtiment 350, Université Paris-Sud, F-91405 Orsay, France

‡ Institute for Experimental Physics, Technical University, A-1040 Vienna, Austria

Received 20 October 1988

Abstract. The electrical resistivities of monocrystalline Tm and of the solid solutions α-TmH_x, $x \leq 0.1$, have been measured along the c axis and the b axis in the temperature range $2\,K \leq T \leq 300\,K$. The Néel temperature T_N for both orientations and the spin-disorder resistivity $\rho_{mag}^{0,b}$ of the b axis specimens decrease with increasing x, owing to decreasing conduction electron density and weakening RKKY interaction, while the residual resistivity ρ_r^b increases linearly by 4.0(1) $\mu\Omega$ cm (at.%H)$^{-1}$ in solution. For the c axis specimens, one observes a strong non-linear increase in ρ_r^c with increasing x, even suppressing the original diminution in ρ in the ordered state; this is interpreted by an H-induced evolution of the superzone boundaries. The temperature dependence of the magnetic resistivity term $\rho_m^b(T)$ in the basal plane is not easily understood through a simple excitation mechanism but is best fitted through a combination: $\rho_m^b(T) \propto AT^n + BT^2 \exp(-\Delta/kT)$, where the power n and the gap Δ both decrease with increasing x.

1. Introduction

Tm is one of the several rare earths which possess a high solubility of H at low temperatures (α-phase) up to 11 at.% H per metal atom. The influence of hydrogen on the magnetic properties of polycrystalline Tm has been investigated by electrical resistivity (Daou *et al* 1980, 1981a), magnetisation (Daou *et al* 1981b, Ito *et al* 1984) and neutron diffraction measurements (Daou *et al* 1983), and a review has been presented by Vajda and Daou (1984). It had been found that both the transition temperature T_N (=57.7 K for pure Tm) to the antiferromagnetic sinusoidal c-axis-modulated (CAM) structure and the transition temperature T_C (=39 K in Tm) to the seven-layer 'ferrimagnetic' (three spins up and four spins down along the c axis) structure decreased by roughly 1 K (at.% H)$^{-1}$ in solution. In addition, the spin-disorder resistivity ρ_{mag}^0 and the paramagnetic Curie temperature θ_p also decreased steadily with increasing H content. All these findings were satisfactorily explained by a depopulation of the conduction band through H, thus weakening the RKKY interaction.

On the contrary, a similar study of the system α-ErH_x has shown strong anisotropy effects on single crystals (Vajda *et al* 1987), which had in part been attributed to the effects of a uniaxially ordered H configuration at low temperatures, namely H–H pairs on second-neighbour tetrahedral sites along the c axis. (This had been established by diffuse neutron scattering on the analogous system α-LuD_x by Blaschko *et al* (1985).) In

0953-8984/89/264099 + 11 $02.50

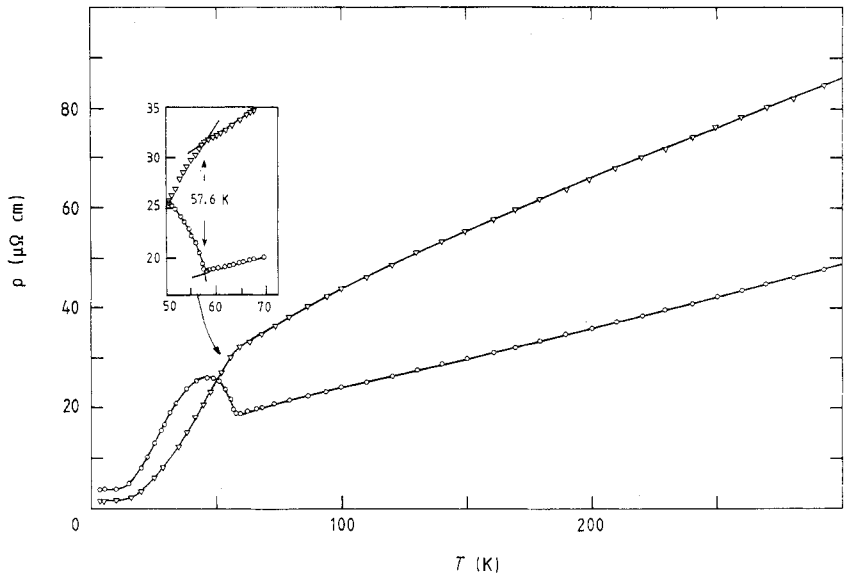

Figure 1. Temperature dependence of the resistivity of Tm single crystals parallel to b (▽) and to c (○). The inset shows the region around the antiferromagnetic transition temperature T_N.

particular, a modification of the superzone boundaries associated with the sinusoidal and helicoidal spin structures of Er had been observed, as well as a gap-like behaviour in the spin-wave spectrum of its cone structure—in contradiction with theory. It was, therefore, interesting to start a similar investigation on monocrystalline Tm, in view of its strongly anisotropic magnetic structure and the equally anisotropic H configuration below about 170–200 K. In this paper, we present resistivity measurements on single crystals of α-TmH_x along the b axis and the c axis†, while a parallel study of their magnetisation has been conducted in collaboration with the Service National des Champs Intenses at Grenoble.

2. Experimental procedure

The specimens were prepared from a 4 g single crystal grown by the Ames Laboratories (Ames, Iowa, USA) from arc-melted Tm, with the major (more than 1 at.%) substitutional impurities: 25 at.ppm Fe, 11 at.ppm Cu, 10 at.ppm Cl, 8 at.ppm Ce, 3 at.ppm Sc, 3 at.ppm La, 3 at.ppm Si, 3 at.ppm Ca, 3 at.ppm K and 3 at.ppm Na and the gaseous impurities 380 at.ppm C, 340 at.ppm H, 125 at.ppm F, 24 at.ppm N and 10 at.ppm O. Three specimens were cut from this crystal and provided with spot-welded Pt leads for resistance measurements: one with the large dimension parallel to the c axis measuring 8 mm × 1.2 mm × 1.1 mm, and the two others parallel to the b axis measuring 6.8 mm × 0.9 mm × 0.9 mm and 6.8 mm × 0.85 mm × 0.85 mm, respectively. The crystals were first investigated in the pure state and then loaded successively with H at 500 °C to obtain the following concentrations x: parallel to c, 0.03, 0.05, 0.056, 0.078

† Preliminary data were in part reported at the International Conference on Magnetism, Paris, July 1988, Poster 4PJ-14.

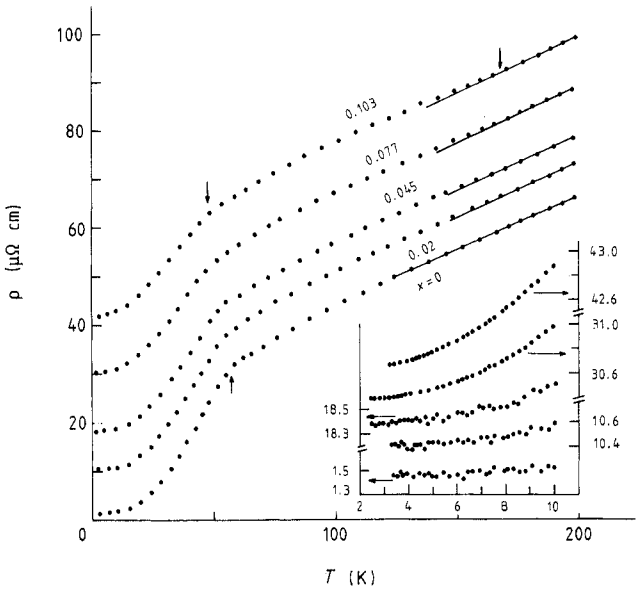

Figure 2. Temperature dependence of the resistivity of TmH_x crystals parallel to the b axis for a selected set of x. The arrows indicate T_N and the structural anomaly near 170 K. The inset shows the low-T part, demonstrating the growing importance of the magnetic excitations with x.

and 0.10 atoms H/atoms Tm; parallel to b, 0.008, 0.012, 0.02, 0.045, 0.07, 0.077, 0.087, 0.09, 0.10 and 0.103 atoms H/atoms Tm. By using the same starting crystals for many of the loaded specimens, we greatly reduce the errors due to the geometrical shape factor determination. The electrical measurements were made in a pumped liquid-He cryostat between 2 and 300 K, with automatic data acquisition and treatment; details can be found for example in the paper by Vajda *et al* (1987).

3. Experimental results

Figure 1 shows the thermal dependence of the electrical resistivity for two pure Tm crystals along the principal axes serving as a base for the H-loaded crystals. The results are in very good agreement with the original data of Edwards and Legvold (1968), in particular the antiferromagnetic transition temperature T_N (see inset of figure 1) of 57.6(2) K, which is somewhat higher than the value of 56 K usually given in the literature (see, e.g., Coqblin 1977) and probably indicating some residual H (1–2 at.%) in their specimens. The high-temperature slopes of the resistivities read in the interval $200\ K \leqslant T \leqslant 300\ K$ from figure 1 of Edwards and Legvold (1968) are within 5% of the values in our work, but the $(d\rho^b/dT)/(d\rho^c/dT)$ ratio of 1.97 given by them is inexplicably higher than our 1.50. On the contrary, if we take the slopes in the interval $100\ K \leqslant T \leqslant 160\ K$ (as has been done in order to avoid the magnetic fluctuations just above T_N but to remain in the frozen state of the H atoms for TmH_x), then one gets $d\rho^b/dT = 0.229$ and $d\rho^c/dT = 0.118\ \mu\Omega\ cm\ K^{-1}$, with a ratio of 1.94.

In figure 2, we present a selection of data from H-loaded crystals parallel to the b axis showing a steady increase in the residual resistivity and a decrease in T_N. An

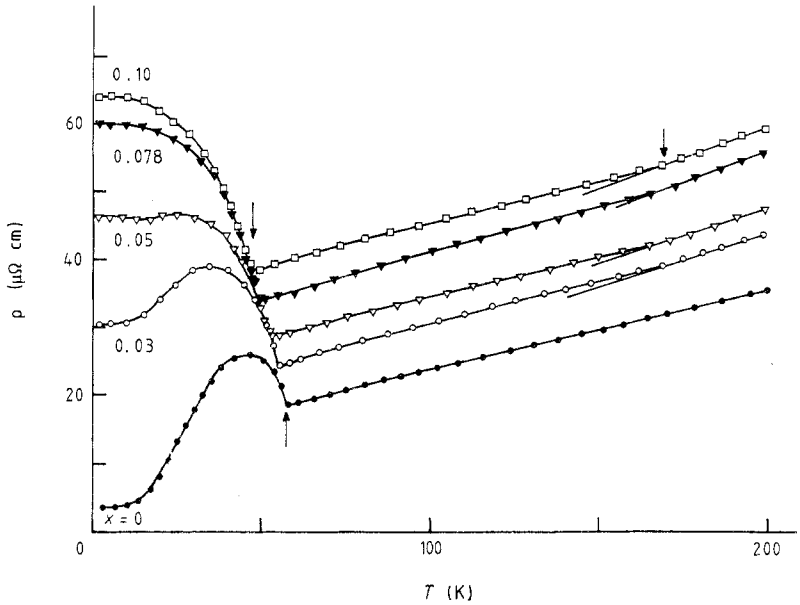

Figure 3. Same as for figure 2, for *c* axis crystals.

interesting phenomenon is demonstrated in an enlarged view in the inset; the low-temperature part of $\rho(T)$ up to about 10 K is almost constant for pure Tm, showing the insignificance of thermally excited processes such as phonons or magnons, but this is no longer true for crystals with $x > 0$; the thermal growth of the resistivity begins ever earlier with increasing x such that for example the $TmH_{0.103}$ crystal has not yet reached its residual value at 3 K. Finally, we note the anomaly due to H ordering, which is manifested as a slope change near 170 K. As to the ferromagnetic transition at T_C, it is not easily observable in the resistivity measurements; it had been noted (Daou *et al* 1980) that the slope maximum in the low-temperature region of polycrystalline Tm corresponded closely to the T_C as measured by neutron diffraction or magnetisation; taking this into account, it seems that T_C of the *b* axis crystals also decreases with increasing x.

The thermal dependence of the resistivities of the *c* axis crystals for a series of H concentrations is plotted in figure 3. One notes—as for the *b* axis crystals—the decrease in T_N and the anomaly near 170 K but, in addition, we have a pronounced evolution of the whole low-temperature part of $\rho(T)$ below T_N. In fact, the residual resistivity increases with increasing x so strongly that the resistivity drop due to magnetic ordering below about 35 K is no longer observable for $x \geqslant 0.05$ and $\rho(T)$ remains steadily increasing with decreasing temperature, preventing the manifestation of ρ_{mag} from being seen.

We have summarised in table 1 the relevant data concerning the residual resistivity, the room-temperature resistivity and the slopes in the region $100 \leqslant T \leqslant 160$ K, as well as T_N and the spin-disorder resistivity ρ^0_{mag} determined through extrapolation of the T-dependence of ρ between 100 and 160 K (to avoid the break at the 170 K anomaly) to zero. Figure 4 shows the x-dependence of T_N for both orientations and those of ρ^0_{mag} and ρ_r for the *b* axis crystals only. Their rather linear evolution with x should be noted—T_N decreases by 1.0(1) K (at.% H)$^{-1}$, $\rho^{0,b}_{mag}$ by 0.5(1) $\mu\Omega$ cm (at.% H)$^{-1}$, and ρ^b_r increases by 4.0(1) $\mu\Omega$ cm (at.% H)$^{-1}$, the latter value being thus the specific H resistivity ρ^{Tm}_H in solution in thulium.

Table 1. Specimen characteristics.

x (atoms H/atoms Tm)	ρ_r ($\mu\Omega$ cm)	ρ_{293K} ($\mu\Omega$ cm)	$d\rho/dT$ [a] ($\mu\Omega$ cm K^{-1})	ρ^0_{mag} [b] ($\mu\Omega$ cm)	T_N (K)
		Parallel to c			
0	3.55	47.7	0.118	8.5	57.6
0.03	30.5	57.65	0.133	—	54.6
0.05	46.25	61.5	0.120	—	52.4
0.056	49.65	65.3	0.129	—	51.8
0.078	60.0	71.9	0.133	—	49.6
0.10	64.0	75.0	0.121	—	47.3
		Parallel to b			
0	1.47	84.5	0.229	19.5	57.8
0.008	4.40	87.9	0.232	19.2	(56.3)[c]
0.012	5.30	87.2	0.228	18.6	(56.1)
0.02	10.4	91.25	0.224	18.1	55.7
0.045	18.35	96.65	0.217	16.95	52.6
0.07	26.15	104.15	0.215	16.35	50.4
0.077	30.4	107.25	0.212	15.55	49.4
0.087	36.05	112.9	0.212	15.35	48.2
0.09	34.15	109.8	0.210	14.5	(48.0)
0.10	44.8	117.0	0.199	13.8	46.7
0.103	42.0	118.3	0.210	14.6	46.9

[a] Determined in the interval $100\ K \leqslant T \leqslant 160\ K$.

[b] Determined through extrapolation of $\rho(T)$ from the region $100\ K \leqslant T \leqslant 160\ K$ to 0 K and subtraction of ρ_r.

[c] The crystals with the Néel temperature given in parentheses had their x determined *a posteriori* from the measured T_N.

4. Data analysis

The thermal increase in the resistivity with increasing T below about 50 K is due to magnetic and to phonon excitations and can be analysed accordingly:

$$\rho_{tot}(T) = \rho_r + \rho_{mag}(T) + \rho_{ph}(T). \tag{1}$$

We have seen, in particular in the inset of figure 2, that $\rho(T)$ for TmH_x crystals with high x does not exhibit a constant (residual) value down to the lowest measured temperatures. We have estimated the phonon contribution (using a Debye temperature $\theta_D = 138$ K, determined by Hilscher *et al* (1989), and the measured high-temperature slopes of $\rho(T)$) to 0.3 $\mu\Omega$ cm at 20 K and less than 0.1 $\mu\Omega$ at 10 K in the case of the b axis crystals and even less for the c axis, which means that the magnetic contribution to $\rho(T)$ is overwhelming. Therefore, considering the strongly anisotropic nature of the magnetism of Tm we have tried to fit an exponential expression to $\rho_{mag}(T)$ of the form

$$\rho_{mag} \propto T^2 \exp(-\Delta/kT) \tag{2}$$

which is represented as an Arrhenius plot in figure 5; Δ is the excitation gap in the spin-wave spectrum. We note that, for pure Tm, the fit is reasonable over more than one decade, in the interval 8–22 K, giving a gap of $\Delta/k = 37.7$ K. For the hydrogenated samples, the fit is less satisfactory, but it is clear that the slopes, i.e. Δ, strongly decrease with increasing x: down to $\Delta/k = 6$ K for $TmH_{0.10}$. In figure 6, we have collected the

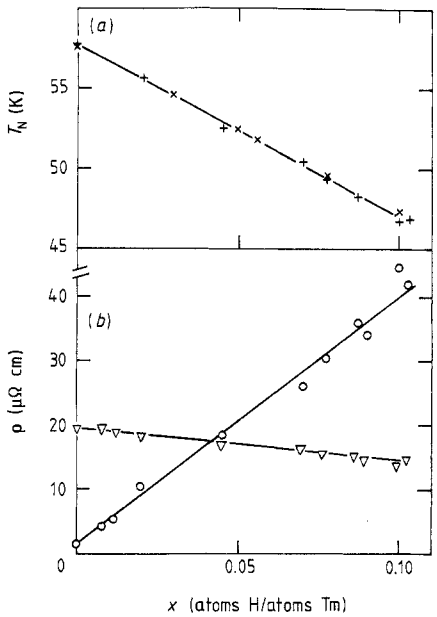

Figure 4. (*a*) Variation in T_N with hydrogen concentration x for crystals parallel to the b axis (+) and to the c axis (×). (*b*) Variations in the residual resistivity ρ_r^b (○) and in the spin-disorder resistivity $\rho_{mag}^{0,b}$ (▽) as functions of x for b axis crystals.

values for Δ/k of all b axis crystals and of the two c axis crystals which exhibit a decreasing $\rho(T)$ below T_N, $x = 0$ and $x = 0.03$. An extrapolation to higher x indicates the disappearance of the gap towards $x \simeq 0.15$. We should also mention here that a parallel study of the specific heat of α-TmH_x in the magnetic range allowed us to fit the magnetic term $c_m \propto T^{3/2} \exp(-\Delta/kT)$ with a gap of $\Delta/k = 43$ K (Hilscher *et al* 1989), in good agreement with the present data, while the fit became very poor for $x > 0$.

We then attempted to analyse the low-temperature data with a power function AT^n for the intrinsic resistivity $\rho_{int} = \rho_{tot}(T) - \rho_r$ (ρ_{ph} is negligible in this T range), exhibited in figure 7 for a selected set of b axis specimens. The straight-line fit works reasonably well for more than two orders of magnitude up to 15–20 K, with a strongly decreasing power n with increasing x (shown in the inset for all measured concentrations): $n \simeq 5$–2.45. At the same time, the coefficient A increases, leading to a growing contribution of ρ_{mag} at low temperatures as seen in figure 2. For high temperatures, one observes a deviation from the linear fit, the curves joining each other near T_N.

To analyse the c axis resistivity (figure 3), we attribute the increase in ρ below T_N to the manifestations of new magnetic superzones produced by periodic structures along the c axis. Thus, following the Elliott–Wedgwood (1963) theory, the total resistivity ρ_{tot}^0 is modified by superzone boundary scattering to become

$$\rho_{tot} = \rho_{tot}^0/(1 - \delta M) \tag{3}$$

where M is the order parameter for sinusoidal ordering along c and δ is related to the gap amplitude of the superzone boundaries. Comparing the (non-modulated) b axis data with the c axis data, one can determine δM from the measured ratios of the

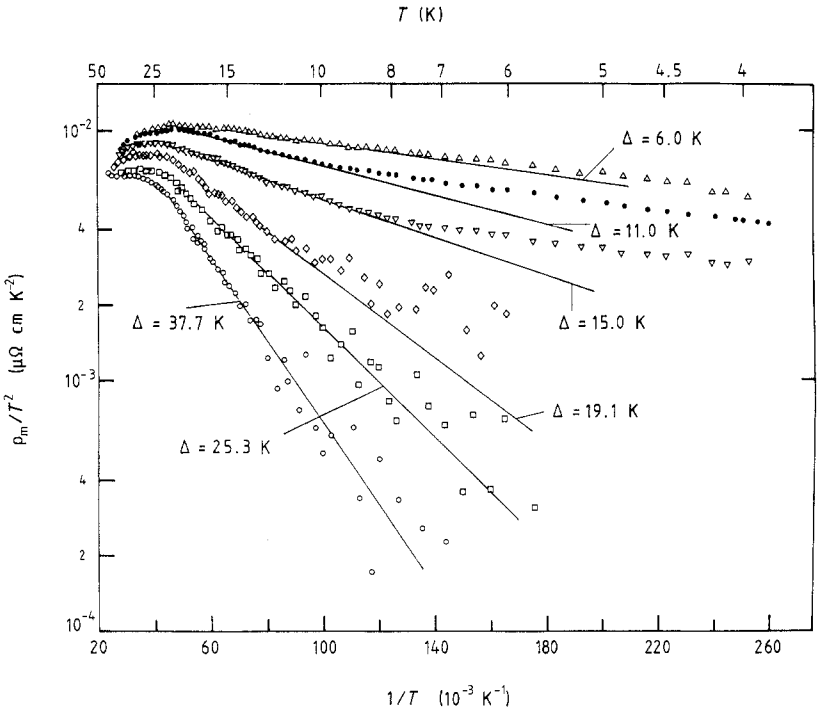

Figure 5. Arrhenius plot of the magnetic resistivity $\rho_{mag}(T)/T^2$, for several b axis crystals: ○, $x = 0$; □, $x = 0.02$; ◇, $x = 0.045$; ▽, $x = 0.07$; ●, $x = 0.087$; △, $x = 0.10$. The slopes give the value Δ/k of the magnon gap, which decreases with increasing x.

respective high-temperature slopes and residual resistivities ρ_r (from table 1) such that

$$(d\rho^b/dT)/(d\rho^c/dT) = (\rho_r^b/\rho_r^c)/(1 - \delta M). \tag{4}$$

We have given the corresponding data in table 2 and plotted them in figure 8; one notes a decreasing tendency for δM as a function of x which becomes stronger for higher concentrations. For pure Tm, our value for $\delta M = 0.79$ compares favourably with the δM of 0.86 determined by Edwards and Legvold (1968), while Elliott and Wedgwood (1963) had predicted a theoretical value of 0.29.

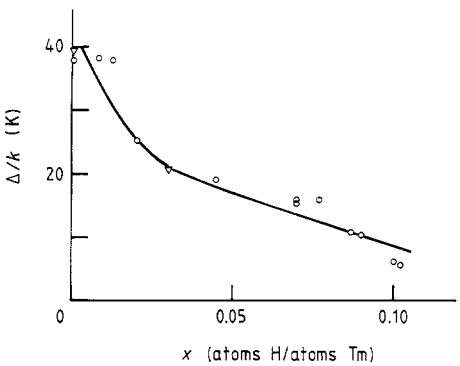

Figure 6. The gap Δ/k in the magnon spectrum as a function of x, for all b axis crystals (○) and two c axis crystals (▽).

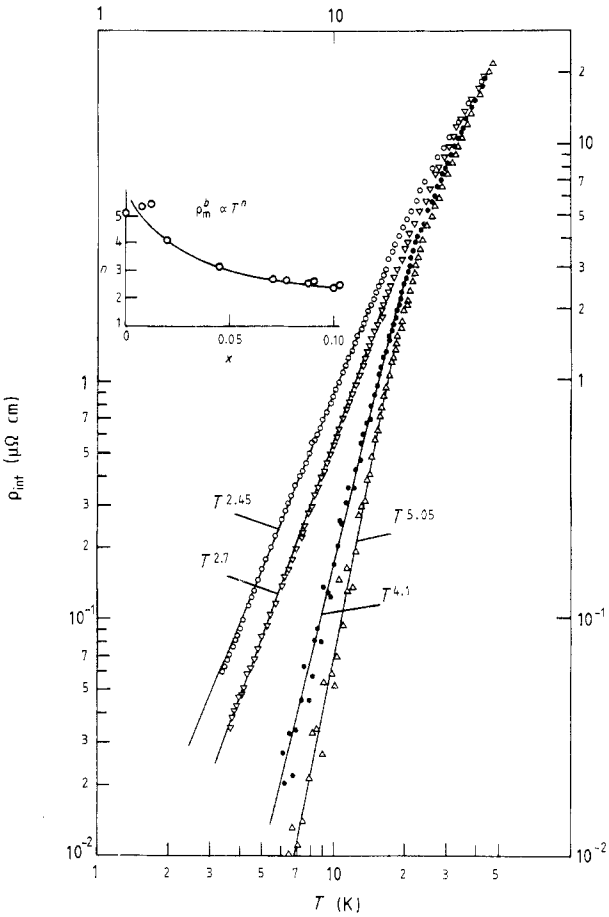

Figure 7. Temperature dependence of the intrinsic resistivity $\rho_{int} = \rho_{tot} - \rho_r$ in a double-logarithmic plot for several *b* axis crystals: △, $x = 0$; ●, $x = 0.02$; ▽, $x = 0.07$; ○, $x = 0.103$. The inset shows the exponent n of the power functions AT^n used to fit the experimental data, for all measured H concentrations.

5. Discussion

As already mentioned in § 1, the decreases in the antiferromagnetic transition temperature T_N and in the spin-disorder resistivity ρ^0_{mag} with increasing H concentration x can be understood through an electronic mechanism—a decrease in the density n_F of states at the Fermi surface and, generally, a decrease in the number of carriers responsible for the RKKY interaction. Thus, in the molecular-field approximation, one can write

$$\begin{aligned} kT_N &= \tfrac{2}{3}I(Q)(g_J-1)^2J(J+1) - \tfrac{4}{15}D(S-\tfrac{1}{2})(S+\tfrac{3}{2}) \\ \rho^0_{mag} &= (\hbar k_F/2\pi z)(m^*\Gamma/e\hbar^2)^2(g_J-1)^2J(J+1) \end{aligned} \tag{5}$$

where the exchange integral $I(Q)$ is proportional to $z^2m^*\Gamma^2/k_F^2$ (z is the number of conduction electrons per atom, Γ the exchange interaction parameter, m^* the effective mass and k_F the Fermi wavevector), $J = L + S$ is the total angular momentum and D is the anisotropy coefficient. In this model, the effect of H would be the formation of low-

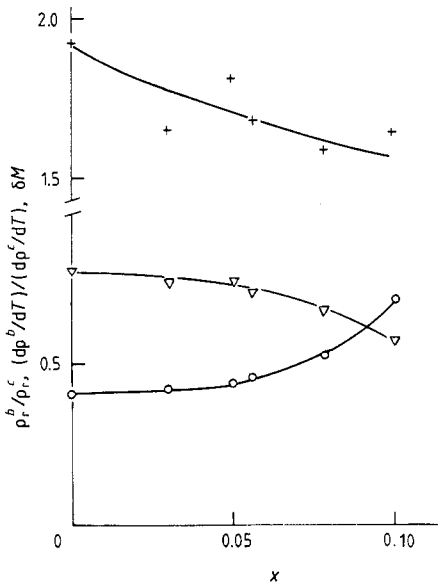

Figure 8. The ratios ρ_r^b/ρ_r^c (○) and $(d\rho^b/dT)/(d\rho^c/dT)$ (×) (in the interval $100\ K \leqslant T \leqslant 160\ K$) used to determine the gap δM (▽) of the superzone boundaries perpendicular to the c axis, for all measured crystals TmH_x.

Table 2. Determination of the superzone gap for the c crystals.

x (atoms H/atoms Tm)	ρ_r^b/ρ_r^c	$(d\rho^b/dT)/(d\rho^c/dT)$ [a]	δM [b]
0	0.41	1.94	0.79
0.03	0.42	1.65	0.75
0.05	0.44	1.81	0.76
0.056	0.46	1.68	0.72_5
0.078	0.53	1.59	0.67
0.10	0.70	1.64	0.57

[a] Determined from the values given in table 1, with occasional interpolation for several b crystals.
[b] Determined from equation (4).

energy metal–H bonding states pumping electrons from the conduction band. These findings agree with all earlier observations on polycrystalline material and are independent of the crystal orientation.

The situation appears to be somewhat more complicated when one considers the temperature dependence of the magnetic contribution to the resistivity $\rho_{mag}(T)$ for various H concentrations (figures 5 and 7). Indeed, it seems that, at the lowest temperatures, a power fit AT^n agrees best with the experimental data while, in the intermediate range $10 \leqslant T \leqslant 25\ K$, an exponential fit is more appropriate. Thus, a combination of the two dependences, in the form

$$\rho_{mag}(T) = AT^n + BT^2 \exp(-\Delta/kT)$$

would possibly work best, the two terms being representative of two temperature

regimes. The magnetic resistivity is essentially dominated by spin waves, which behave as $T^2\exp(-\Delta/kT)$ in anisotropic ferromagnets (cf e.g. Coqblin 1977), where Δ is the energy gap in the spin-wave spectrum. At low temperatures ($T \ll \Delta/k$), this term disappears and one observes a predominance of the power law, possibly signifying the presence of an antiferromagnetic excitation. We have found for pure Tm a gap $\Delta/k \simeq$ 38 K, this value decreasing with increasing x down to 6 K for $TmH_{0.10}$. This would explain why simultaneously the validity regime of the exponential law decreases in favour of that of the power law; we wish to recall here that the exponential fit of the specific heat data by Hilscher *et al* (1989), giving a Δ/k of 43 K for pure Tm, also lost its validity in the case of the hydrogenated specimens. As to the x dependence of the gap Δ, it is reasonable to relate it to a diminishing anisotropy of the system with increasing x. In fact, it has been shown (Bonnet and Daou 1979) that H in solution expands the Tm lattice relatively stronger in the c than in the a direction, driving the originally distorted structure ($c/a = 1.57$) closer to the ideal HCP c/a ratio of 1.63. This latter phenomenon itself is probably due to the uniaxially ordered H configuration predominant at low temperatures (cf § 1).

On the contrary, recent work on the study of magnetic excitations in Tm (McEwen and Steigenberger 1988) by neutron spectroscopy has revealed three modes in the ferromagnetic phase, the lowest with an energy of around 3.5–4 meV corresponding well to the value of our gap. McEwen and Steigenberger interpret their results in terms of a crystal-field level scheme, but the description does not seem straightforward. Furthermore, preliminary measurements of the magnetisation of α-TmH_x single crystals made in collaboration with G Chouteau (SNCI, Grenoble) disclosed below 4.2 K a not yet resolved complex structure which becomes more pronounced as the H content increases. Additional neutron scattering work seems indicated, but it is clear, in any case, that there is a strong anisotropic interaction between the dissolved H (eventually in pairs) and the magnetic structures.

Finally, we shall discuss the most spectacular aspect of the experimental results—the modification with H of the influence of the superzone boundaries upon the c axis resistivity below T_N (cf figure 3). We have seen that the measured data of the residual resistivity can be understood when applying equation (4) with a varying superzone gap δM. First, this will give values for the 'real' ρ_r^c—in the absence of superzone boundaries—by multiplying by $1 - \delta M$; for pure Tm, one obtains using tables 1 and 2

$$\rho_r^c(\mathrm{Tm}) = 3.55(1 - 0.79) = 0.75\ \mu\Omega\ \mathrm{cm}.$$

This leads then also to a modified spin-disorder resistivity following the extrapolation to 0 K and subtraction of ρ_r^c:

$$\rho_{mag}^{0,c}(\mathrm{Tm}) = 11.3\ \mu\Omega\ \mathrm{cm}.$$

Comparing with the Legvold (1972) formula (which relates the residual resistivities, the spin-disorder resistivities and the phonon resistivities in various crystal directions to the Fermi surface anisotropy)

$$\rho_r^b/\rho_r^c = (\mathrm{d}\rho^b/\mathrm{d}T)/(\mathrm{d}\rho^c/\mathrm{d}T) = \rho_{mag}^{0,b}/\rho_{mag}^{0,c} = \int_{E_F} \mathrm{d}S_c \Big/ \int_{E_F} \mathrm{d}S_b \qquad (6)$$

where the last term is the reciprocal ratio of the Fermi surface projections in the

corresponding directions, we obtain for the superzone-corrected ratio of ρ^0_{mag} in pure Tm

$$\rho^{0,b}_{mag}/\rho^{0,c}_{mag}(Tm) = 1.73$$

while we found that $(d\rho^b/dT)/(d\rho^c/dT) = 1.94$. (The corrected ratio ρ^b_r/ρ^c_r had been chosen *a priori* equal to $(d\rho^b/dT)/(d\rho^c/dT)$ in order to be able to calculate δM.) The ratio of the Fermi surface integrals has been evaluated by Legvold (1972) theoretically to give a value of 2 which, together with the above-determined ratios, is quite satisfactory. One can also calculate the superzone-corrected $\rho^{0,c}_{mag}$ for the hydrogenated specimens using equation (1), the modified $\rho^c_r(1 - \delta M)$ and an estimated ρ^c_{ph}. The precision is not very high, since it is rather sensitive to the exact value of δM; thus, we obtain, for $TmH_{0.10}$, $\rho^{0,c}_{mag} = 7.5 \pm 1\ \mu\Omega$ cm, showing a similar decreasing dependence on x as $\rho^{0,b}_{mag}$ and giving

$$\rho^{0,b}_{mag}/\rho^{0,c}_{mag}(TmH_{0.10}) = 1.9.$$

The decrease in the superzone gap amplitude δM with increasing H concentration (figure 8) might be related to the simultaneous decrease in the exchange interaction constant Γ or in the magnetic moment M or to both; the latter is also supported by results from susceptibility (Daou *et al* 1981b) and neutron diffraction measurements (Daou *et al* 1983). All this goes back to a decrease in the conduction electron density, i.e. to the same mechanism that is responsible for the decrease in T_N.

Acknowledgment

We appreciated interesting discussions with B Coqblin.

References

Blaschko O, Krexner G, Daou J N and Vajda P 1985 *Phys. Rev. Lett.* **55** 2876
Bonnet J E and Daou J N 1979 *J. Phys. Chem. Solids* **40** 421
Coqblin B 1977 *The Electronic Structure of Rare Earth Metals and Alloys* (New York: Academic)
Daou J N, Radhakrishna P, Tur R and Vajda P 1981b *J. Phys. F: Met. Phys.* **11** L263
Daou J N, Radhakrishna P, Vajda P and Allain Y 1983 *J. Phys. F: Met. Phys.* **13** 1093
Daou J N, Vajda P, Lucasson A and Lucasson P 1980 *Solid State Commun.* **34** 959; **35** 809
—— 1981a *J. Phys. C: Solid State Phys.* **14** 129
Edwards L R and Legvold S 1968 *Phys. Rev.* **176** 753
Elliott R J and Wedgwood F A 1963 *Proc. Phys. Soc.* **81** 846
Hilscher G, Pillmayr N, Vajda P and Daou J N 1989 to be published
Ito T, Legvold S and Beaudry B J 1984 *Phys. Rev.* B **30** 240
Legvold S 1972 *Magnetic Properties of Rare-Earth Metals* ed. R J Elliott (New York: Plenum)
McEwen K A and Steigenberger U 1988 *Int. Conf. Magnetism (Paris) July 1988* Poster 4PJ-1.
Vajda P and Daou J N 1984 *J. Less-Common Met.* **101** 269
Vajda P, Daou J N, Burger J P, Schmitzer C and Hilscher G 1987 *J. Phys. F: Met. Phys.* **17** 2097